A new look at the Galim (a) and Galim (b) meteorites

MIREILLE CHRISTOPHE MICHEL-LÉVY

Laboratoire de Minéralogie-Cristallographie associé au CNRS, Université Paris 6, 4 Place Jussieu, 75252 Paris, Cedex 05, France

AND

MICHÈLE BOUROT-DENISE

Laboratoire de Minéralogie, Muséum d'Histoire Naturelle, Paris, France

Abstract

Small stones were recovered from a meteorite shower observed in Cameroon on November 13, 1952. The majority are LL6 specimens, Galim (a), but one is a chondrule-rich enstatite chondrite, Galim (b). Petrology and mineral chemistry were determined on polished sections of both types. Galim (a) has undergone multiple brecciation. During the first, chromite apparently recrystallized in healed fractures under more reducing conditions than those which prevailed when the silicates recrystallized. Galim (b) shows some features of petrologic type 3 but differs considerably from the other unequilibrated E chondrites. It is suggested that Galim (a) and Galim (b) belong to the same meteorite shower.

KEYWORDS: meteorite, Galim, meteorite shower, Cameroon, enstatite chondrite.

Introduction

ON November 13, 1952, at 16.50 local time, a highly luminous meteor exploded over a bush region in Cameroon at 12° 26′ E and 7° 3′ N. It must have been a very large object according to the witnesses, but after a double detonation it seems to have fragmented into small stones that fell among cattle in the bush. Only 7 tiny stones (maximum size 3 × 2 cm) were recovered at the time, of which 4 reached the Museum d'Histoire Naturelle in Paris. Three are LL6 brecciated fragments (and supposedly 6 of the 7 pebbles, according to the 1952 report of M. Koch, a geologist who observed the fall from Mayo-Darlé and got stones from the natives); the fourth is an enstatite chondrite. Previous descriptions pointed out the brecciated texture of some pebbles (Jeremine, 1953), and the different nature of the fourth stone (Orcel and Jeremine, 1958) without giving them the proper classification, owing to the lack of chemical analyses. Mason and Wiik (1964) recognized the brecciated stones as an amphoterite (LL group). Recently we re-examined this material and noted that both the LL6, named Galim (a), and the enstatite chondrite, Galim (b), were interesting in their own way, as will be shown hereafter.

Galim (a)

To avoid waste of material, we only studied previously cut thin and polished sections from one or two pebbles representing 7 cm^2. The two stones left untouched (10.8 and 7.7 g respectively) have lost part of their crust, showing their similarity with the investigated material.

The most important characteristic is the multiple brecciation–recrystallization history of this chondrite, because of which the chondrules have been erased, with only a few poorly defined examples remaining. The first recognizable brecciation episode is underlined by the crystallization of chromite along healed fractures (Fig. 1); the second was accompanied by the melting of troilite which invaded all the cracks and had in some places a corrosive effect as can be seen by the rounded outlines of the minerals against the sulphide (Figs. 2 and 3); nickel-iron also fills some cracks but we did not find any veins composed of mixtures of sulphide and FeNi metal. This sulphide recrystallized

Mineralogical Magazine, September 1988, Vol. 52, pp. 519–25

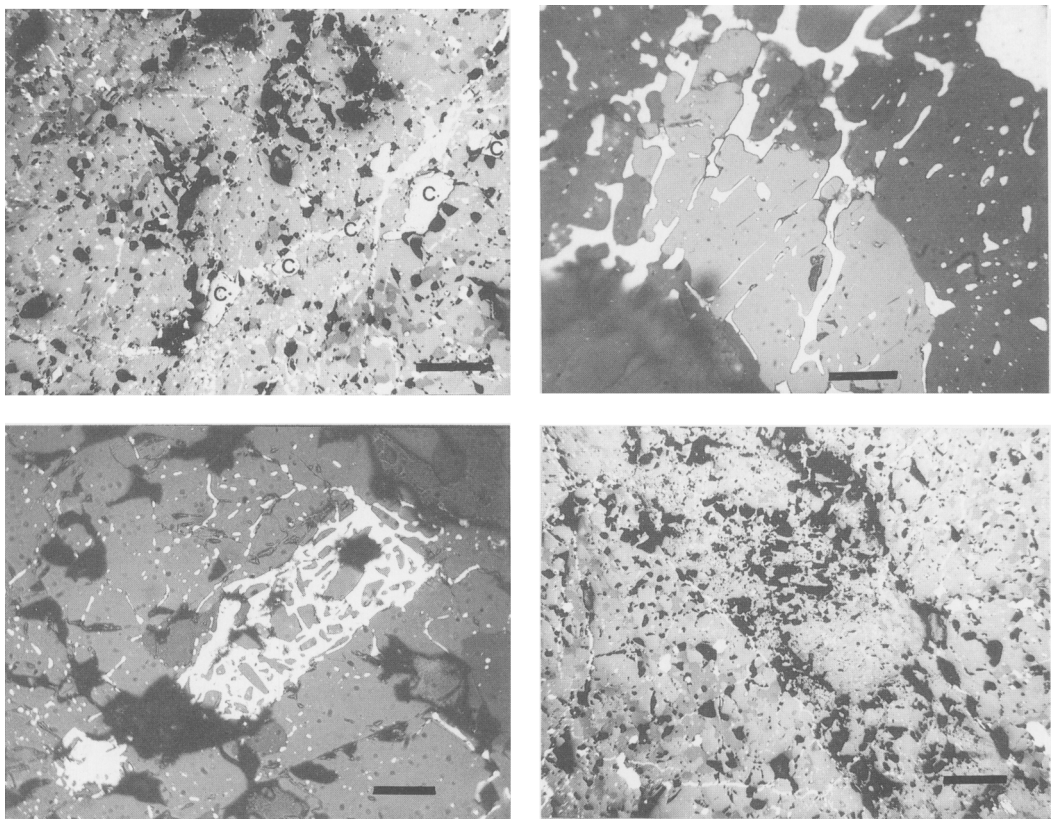

FIGS. 1–4. Photomicrographs of Galim (a). FIG. 1 (*top left*). The oldest brecciation episode is indicated by the crystallization of chromite (C) along healed fractures. White, troïlite; light grey, olivine and pyroxene; dark grey, feldspar; black holes indicate where crystal fragments have been torn out during polishing. Scale bar 500 μm. FIG. 2 (*top right*). Troïlite filling cracks in silicates (dark grey) and chromite (light grey). Scale bar 20 μm. FIG. 3 (*bottom left*). Subrounded silicate debris surrounded by troïlite (white) which penetrates all the minerals. Scale bar 50 μm. FIG. 4 (*bottom right*). The third brecciation episode is illustrated by the obliquely crossing band full of holes and defects between two well-crystallized clasts; troïlite thin veins (white); evidence of the second brecciation episode is visible in the clast on the lower left. Scale bar 500 μm.

quietly: a single optical orientation is noted for nearly all the patches and threads in a single clast.

The last brecciation occurred when the stone was cold and is now easily discernible by the fragmented, broken, deformed material occurring between undisturbed angular to subrounded clasts (Fig. 4).

Mineral chemistry. Representative analyses of the main mineral phases are reported in Table 1. The crystals are homogeneous and there is little variability, as expected for a highly recrystallized chondrite. Phosphates, represented in a few large areas and containing many tiny voids were not analysed.

The *olivines* are Fa_{30} to Fa_{31} with a low (0.06 to 0.08 wt. %) CaO content. The ferrosilite content of *orthopyroxene* is close to 24.7 mol% and the wollastonite is 1.7 ± 0.1 mol %. The composition of the accompanying '*diopside*' ($En_{45.6}Fs_{11.8}Wo_{43.6}$) indicates an equilibrium temperature of 1000 ± 80 °C, using the chart of Kretz (1982). This estimate is normal for an LL6 chondrite.

The distribution coefficient of MnO between ortho- and clinopyroxene is about 2, in the range of equilibrated chondrite and terrestrial metamorphic rocks. That is also the case for the distribution of chromium in both pyroxenes. The *plagioclase feldspar* is $Ab_{0.85}Or_{0.05}An_{0.10}$ as expected for an amphoterite (LL group chondrite). *Chromite* has normal contents of Al_2O_3, Cr_2O_3, V_2O_3 and Mn for an LL chondrite when compared to the data of Bunch *et al.* (1967). TiO_2 is high, corresponding to the very low or null content of Fe^{3+} (Bukovanska

et al., 1983). However, FeO and MgO are notably abnormal as can be seen on Fig. 5. The location of most of the anhedral chromites along lines, presumably ancient fractures (Fig. 1), suggests that these chromites were mobile and crystallized when the physicochemical conditions were different from those that existed when the silicates recrystallized. The oxygen fugacity may have been lowered compared with that which prevailed earlier when the silicates crystallized.

The *metal* also seems to have been redistributed, there being only a few irregularly scattered nickel-iron grains; all are nickel-rich taenites of nearly uniform composition. The fifteen grains analysed have mean contents of 42% Ni and 1.68% Co.

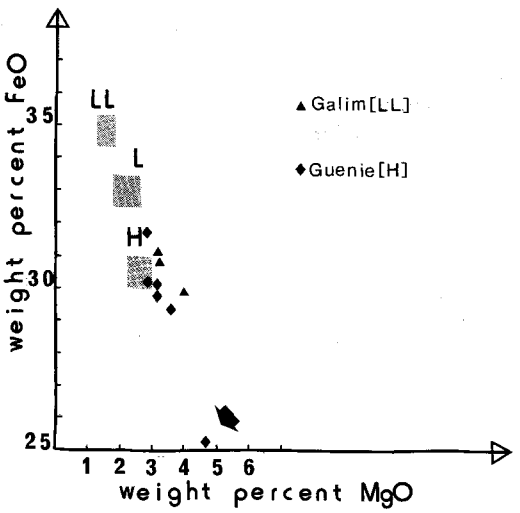

FIG. 5. FeO *vs.* MgO in chromites. Ordinary chondrite groups are indicated. In the H4 chondrite Guénie, chromites enclosed in kamacite (arrow) are different from the normal H-group composition. The Galim (a) chromites have compositions near that of H group chromites, probably indicating more reducing conditions compared with those obtaining during recrystallization of the silicates.

Table 1. Some Galim LL minerals

	Ol	Opx	Cpx	Chr
SiO_2	37.19	55.58	53.94	-
TiO_2	0.02	0.20	0.47	4.20
Al_2O_3	-	0.15	0.53	5.28
Cr_2O_3	0.04	0.11	0.86	55.38
V_2O_3	n.d	n.d	n.d	0.78
FeO	27.94	15.96	6.64	30.88
MgO	35.03	27.25	15.92	3.18
MnO	0.40	0.43	0.20	0.51
CaO	0.08	0.93	20.93	-
Na_2O	-	-	0.60	-
Σ	100.70	100.60	100.10	100.21

Table 2. Some Galim E minerals

	1	2	3	4	5
SiO_2	59.43	57.26	98.23	94.10	69.19
TiO_2	0.04	0.72	0.01	0.03	0.03
Al_2O_3	0.18	2.08	0.11	0.15	18.86
Cr_2O_3	0.11	0.13	-	-	-
FeO	1.42	6.08	0.50	0.81	0.52
MgO	38.03	33.67	-	4.25	0.09
MnO	0.15	0.26	-	0.03	0.01
CaO	0.18	0.49	-	0.07	0.02
Na_2O	-	0.11	0.06	0.08	10.10
K_2O	-	0.01	0.02	-	2.06
Σ	99.54	100.81	98.93	99.52	100.88

1. typical px
2. px rimming the silica chondrule ana.4
3.4. silica-rich chondrules
5. feldspathic composition $Ab_{88}Or_{12}$

Galim (b)

The study was performed on a polished section one centimetre wide and on an old covered thin section.

In the covered thin section, chondrules are identifiable and we note the absence of olivine and orthopyroxene: all pyroxenes are clino- or striated ones. The abundance of metal and troilite renders the matrix opaque, especially since the section is 40 μm thick, but the polished section shows that the rather coarse silicate portion of the matrix is chiefly composed of clastic sub-rounded debris and pyroxene laths; there is little micrometre-sized material and that is enclosed in sulphide grains. The opaque phases are represented by nickel-iron, which occurs as chondrules and irregular grains enclosing pyroxene laths and silica blebs, and by troilite and schreibersite, plus two tiny inclusions of an iron-manganese-zinc sulphide in a large pyroxene crystal. No other unusual minerals specific to enstatite chondrites, nor graphite, were found. The diameters of 152 spherical silicate chondrules range from 50 to 800 μm (20% <

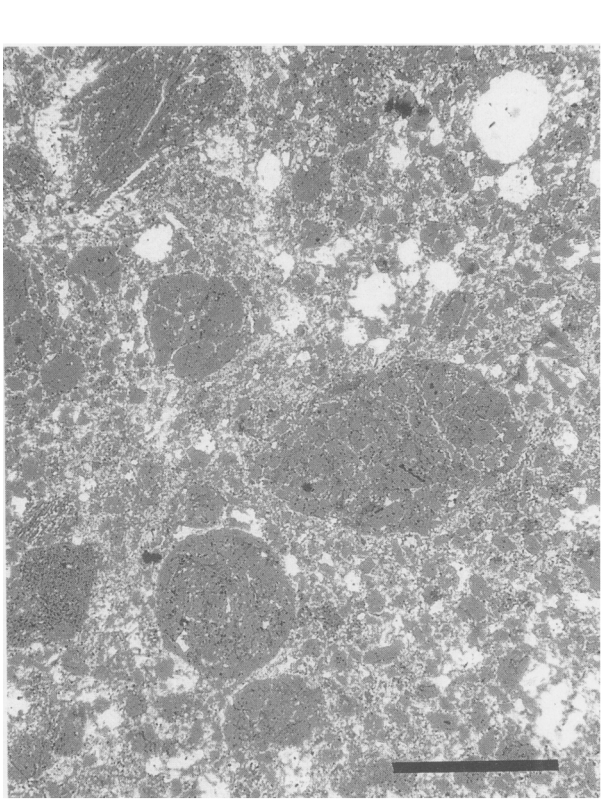

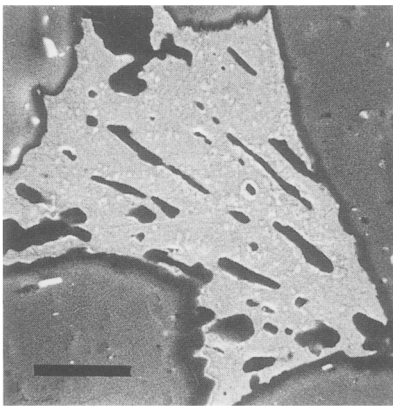

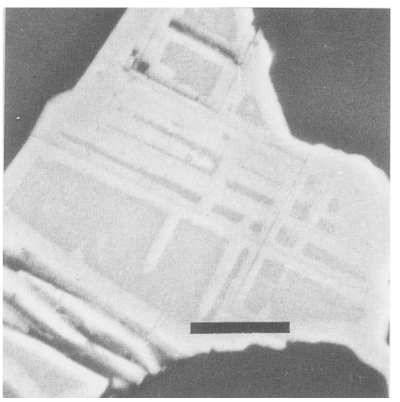

FIGS. 6–8. Photomicrographs of Galim (b). FIG. 6 (*left*). Textural illustration of Galim (b). Chondrules and rock fragments (black) are well delineated. Silicate debris, metal and troïlite make up the matrix. Scale bar 1 mm. FIG. 7 (*top right*). The mesostasis of a large chondrule, made of albitic needles (dark) embedded in kamacite. SEM—Scale bar 20 μm. FIG. 8 (*bottom right*). Cloudy taenite, with grid pattern, between enstatite laths inside another chondrule, lightly etched. SEM—Scale bar 5 μm.

125 μm; 67% between 125 and 500 μm; 13% > 500 μm). All silica-rich chondrules are smaller than 250 μm; the largest rounded rock fragment reaches 1.2 mm. Metallic chondrules range up to 370 μm in diameter. All are composed of kamacite; taenite and troilite when present only occurring at their margin (Fig. 6).

Mineral chemistry. The various phases were analysed by microprobe. A single population of *clino-enstatite* crystals is represented but with a rather wide variation of FeO content, from 0.76 to 6.08 wt. %. Peak values are 1.5% FeO, 0.13% CaO, 0.15% Al_2O_3, 0.12% MnO and < 0.05% for Na_2O, Cr_2O_3 and TiO_2. Crystals in chondrules and matrix have a similar compositional range but the thin pyroxene rims of highly siliceous chondrules are somewhat different (see Table 2). We have found no olivine. This is consistent with the presence of silica-rich chondrules and tiny silica crystals embedded in kamacite, indicating that the chondrules formed from a silica-saturated medium. We wonder whether these chondrules, which are often full of troilite blebs, are glassy or partly crystalline because they have only been observed on the polished section and as their chemical composition is somewhat variable (anal. 3 and 4, Table 2, for example). They are very poor in alkalis unlike the material [albite, anorthoclase or glass (?), anal. 5 and Fig. 7] filling, with or without kamacite and/or troilite, the interstices between the pyroxene laths in the chondrules. K_2O may vary from 0.6 to 4% in the same chondrule, Na_2O changing accordingly.

Kamacite is the main metallic phase, and the only one occurring in spheroids, with Ni contents from 5.6 to 7.5% and Co from 0.44 to 0.89%. Some interstitial kamacite may have a lower Ni content of

4.92% and a Co content of up to 1.53% has occasionally been found. Si is present at a very low level for an enstatite chondrite ($\leqslant 0.01\%$) and P is less than 0.06%. However, a silicon distribution image shows the presence of a thin rim enriched in silica around a kamacite spheroid that presumably resulted from the oxidation of Si-bearing kamacite. There is little *taenite* but it occurs in two different places and in two different varieties; in a few pyroxene chondrules, cloudy taenite is sometimes present with Ni around 34% at the centre of the area (Fig. 8). Tetrataenite is found in the matrix with 49–50% Ni and less than 0.22% Co, most often enclosing rounded cores of kamacite. A little Cu (0.18%) is present in it, and also in small crystals of schreibersite which are nickel-rich ($Ni_{1.8}Fe_{1.2}P$), and have a constant nickel content whenever close to kamacite alone, or between kamacite and taenite.

Table 3. Bulk analyses of Galim (b)

	1	2		3	4
Si	19.45-19.66	19.58	SiO_2	42.0	41.6
Al	0.85- 1.09	0.95	Al_2O_3	1.80	1.91
Mn	0.06- 0.17	0.11	FeO	0.85	-
Mg	13.45-13.63	13.51	MnO	0.14	0.10
Ca	0.38- 0.47	0.43	MgO	22.5	22.5
Na	0.96- 1.19	1.09	CaO	0.60	0.68
Fe	22.79-33.65	31.50	Na_2O	1.47	1.02
Ni	1.54- 1.84	1.64	Fe	30.84	29.3
Co	0.30- 0.40	0.34	Ni	1.64	1.76
S	5.03- 5.31	5.19	Co	0.34	-
P	0.04- 0.15	0.09	S	5.19	3.50
			P	0.09	-
			SUM	107.46	102.37

1. Range of elemental abundances, three 5 x 4 mm areas in the polished thin-section. SEM with Link energy dispersive system. Analyst: M. Tremblay.

2. Mean composition, from 1.

3. Mean composition, from 1, calculated as oxides, as appropriate. Note the high sum, an artifact of the ZAF correction - see the text.

Editorial note : No. 4 is the mean composition, 66 analyses by wavelength dispersive microprobe, 100 μm diameter electron beam. Analyst: R Hutchison. A ZAF correction was applied separately to the uncorrected concentrations of the oxides and Fe, Ni and S, and the results combined. This procedure takes into account the elemental association within the meteorite and so produces an acceptable total. It cannot be applied to the data obtained by the authors. However, the total area analysed was 0.5 μm^2, or 0.25% of the area of the section so no. 4 may not be representative, but note the similarity with no. 3. The EH classification is confirmed. The "ancient covered thin section" was obtained by the British Museum (Natural History), made into a polished thin-section, BM1987, M.13, and used for the wavelength dispersive analysis. R.H.

Troilite seems to have filled previously existing voids. It is pure, without any significant Cr, Mn or Ti contents which usually occur in the troilite of enstatite chondrites. The only peculiar sulphide found is a manganese- and iron-rich sphalerite, present only as two tiny grains ($< 8\ \mu m$) included in a euhedral enstatite. The analysis (S 33.71, Fe 20.12, Mn 8.69, Zn 29.50, Cu 0.11, Na 0.48, Ni 0.37, Σ 93.01%) has a low sum, presumably because of the small size of the grains.

Chemical composition. The chemical analyses have been performed by EDS with the Link Systems AN 10 000 coupled with an SEM, on three 5 x 4 mm scans of the polished section (1, 2, 3, Table 3). It reveals a good homogeneity of the rock, specially for its silicate and sulphide portion; the metal is less uniformly distributed, as can be observed visually. The ZAF correction procedure is calculated for homogeneous material and not for a juxtaposition of phases, as differences in the electron absorption and emission properties of metal, sulphide and silicates will occur. Therefore, the proportion of silicates is overestimated and the analysis sums up too high (Table 3, no. 3). The Fe/Si ratio may be underestimated, but the Mg/Si ratio is not influenced, Mg and Si belonging wholly to the silicates. This ratio is the one expected for an E chondrite. Cr has not been measured; K and Ti have been, but there is too little for a valuable estimate by this method, and the error must be considered to be high also for P and Mn. Na appears too high relatively to Al, as it is found only in feldspar and glass, not in pyroxene. Ca is low but it corresponds to its low content in pyroxene and feldspar.

Discussion

Comparison between Galim (b) and other enstatite chondrites. The analytical method employed for the bulk analysis is not accurate enough to allow detailed comparisons. However, the Mg/Si atomic ratio of 0.8 is specific of E chondrites and quite different from the ratio of 'forsterite chondrites' and Acapulco type chondrites, always greater than 0.9; the Fe/Si atomic ratio without correction (0.8) plots close to Yamato 69001 and 77370 (Fig. 4 in Weeks and Sears, 1985). If Si is overestimated relative to Fe, the ratio should approach the main EH group, for which the S content is also favourable. In spite of its well-delineated chondrules and the slightly variable composition of its pyroxene, Galim (b) differs from the EH chondrites by the absence of olivine, the presence of taenite, the chemical composition of its kamacite and schreibersite, the common nature of its troilite which is not accompanied by the unusual sulphides

specific to the E chondrites. It cannot be classified either with the types E3 or E4, and would better fit the Cumberland falls chondritic inclusions, but for the absence of olivine.

The significant FeO content of pyroxene, the absence of Si in kamacite (which is correlated with the lack of olivine) and of Ti in troilite reflect only moderately reducing conditions during crystallization. These probably were governed by a low C/O ratio (the absence of graphite is important to note) from chondrule formation (melting episode) until the post-accretional final cooling.

If the crystallochemical state of the pyroxenes and glass signifies a relatively rapid cooling from melts, the final cooling through 300 °C must have been slow, because of the occurrence of tetrataenite, in accordance also with the 50% Ni of schreibersite.

Were Galim (a) and Galim (b) from the same parent body? Obviously, this cannot be ascertained from the data presented here. However, the pebbles are quite fresh. They were gathered by cattle breeders who saw them fall, presumably at the periphery of the strewnfield. M. Koch wondered whether the proportion of dense to light stones would have been different towards the centre of the strewnfield.

It is well known that LL brecciated meteorites may carry exotic clasts such as the H group xenolith in St Mesmin (Pellas, 1973) or the small debris in Piancaldoli (Rubin *et al.*, 1982). Galim (b) may then be interpreted as another case of an exotic clast in an LL group host. However, the chemical composition of the chromite (in the LL stone), which seems to have crystallized following a brecciation episode, indicates that it did so in a more reducing environment than that prevailing when the silicates equilibrated. Thus, there is a possibility that Galim (a) was brought into a more reducing environment when it was still quite hot. Alternatively, the redox conditions on the LL parent body may have been modified by the arrival of reduced E chondritic material, perhaps after a shock event. Here it is worth noting that Galim (b) is presently less reduced than EH or EL material yet the low Mg/Si ratio is consistent with its membership of one of these groups. Without mixing of solids, but in a mixed atmosphere, Galim (a), in the last stages of its cooling, would have evolved towards a more reduced mineralogy and Galim (b) would have found itself in more oxidized conditions than those of normal E chondrites.

We may also note that sulphur was mobilized late in both stones, troilite underlining the second brecciation episode in the LL case, and filling all the interstices of the E chondrite. It is conceivable in that case that the original specific E sulphides were decomposed, except for the sphalerite grains which were included and protected in enstatite, releasing the alkalis which formed aluminosilicates, whilst some calcium, manganese and titanium were lost (and possibly other non-measured elements, such as Cr, Zn, etc.), explaining their low present content.

Conclusion

Until recently, unequilibrated enstatite chondrites were not recognized. Now we have a few specimens that we cannot yet assign to either of the established groups, though Weeks and Sears (1985) show their chemical similarities for siderophile elements with the EH group, while some chalcophile elements and Cr place them in an intermediary situation between EH and EL. The Galim (b) stone has some general features of type 3, where each chondrule retains evidence of a high-temperature melting or near-melting episode followed by a rapid cooling to a few hundred degrees celsius, when accretion occurred together with that of many debris. It surely evolved in a reduced medium, but not on the same scale, so probably not on the same parent body as the other unequilibrated E chondrites.

Some observations indicate that Galim (b) and (a) were brought together on a single planetary object rather early in their history, but this remains an open question until further investigations on these stones are undertaken or other similar cases are found.

Acknowledgements

We thank for their technical support the Service de la Microsonde du Muséum d'Histoire Naturelle; M. Blanc for the SEM study, M. Tremblay for the EDS analyses (u.A. 723 du CNRS). Drs R Hutchison and D. W. Sears are thanked for their useful comments and review of the manuscript.

References

Bukovanska, M., Jakès, P., Pernicka, E., and El Goresy, A. (1983) Usti nad Orlici: A new L6 chondrite from Czechoslovakia. *Meteoritics* **18,** 223–40.

Bunch, T. E., Keil, K., and Snetsinger, K. G. (1967) Chromite composition in relation to chemistry and texture of ordinary chondrites. *Geochim. Cosmochim. Acta* **31,** 1569–82.

Jeremine, E. (1953) Sur une nouvelle chute de météorite au Cameroun. *C. R. Acad. Sci. Paris* **237,** 1740–2.

Kretz, R. (1982) Transfer and exchange equilibria in a portion of the pyroxene quadrilatera as deduced from natural and experimental data. *Geochim. Cosmochim. Acta* **46,** 411–21.

Mason, B., and Wiik, H. B. (1964) The amphoterites and meteorites of similar composition. Ibid. **28,** 533–8.

Orcel, J. and Jeremine, E. (1958) Sur la chondrite de Galim. *83e Congrès des Sociétés Savantes,* 211–17.

Pellas, P. (1973) Irradiation history of grain aggregates in ordinary chondrites. Possible clues to the advanced

stages of accretion. *From plasma to planets.* Wiley, 65-92.

Rubin, A. E., Scott, E. R. D., and Keil, K. (1982) Microchondrule-bearing clast in the Piancaldoli LL3 meteorite: a new kind of type 3 chondrite and its relevance to the history of chondrules. *Geochim. Cosmochim. Acta* **46,** 1763–76.

Weeks, K. S., and Sears, D. W. G. (1985) Chemical and physical studies of type 3 chondrites. V: the enstatite chondrites. Ibid. **49,** 1525–36.

[*Manuscript received 9 January 1987; revised 2 September 1987*]